Science Advances
AAAS

Supplementary Materials for

Processive cleavage of substrate at individual proteolytic active sites of the Lon protease complex

Shanshan Li, Kan-Yen Hsieh, Chiao-I Kuo, Shih-Chieh Su, Kai-Fa Huang, Kaiming Zhang*, Chung-I Chang*

*Corresponding author. Email: kmzhang@ustc.edu.cn (K.Z.); chungi@gate.sinica.edu.tw (C.-I.C)

Published 10 November 2021, *Sci. Adv.* **7**, eabj9537 (2021)
DOI: 10.1126/sciadv.abj9537

This PDF file includes:

Supplementary figure legends and tables

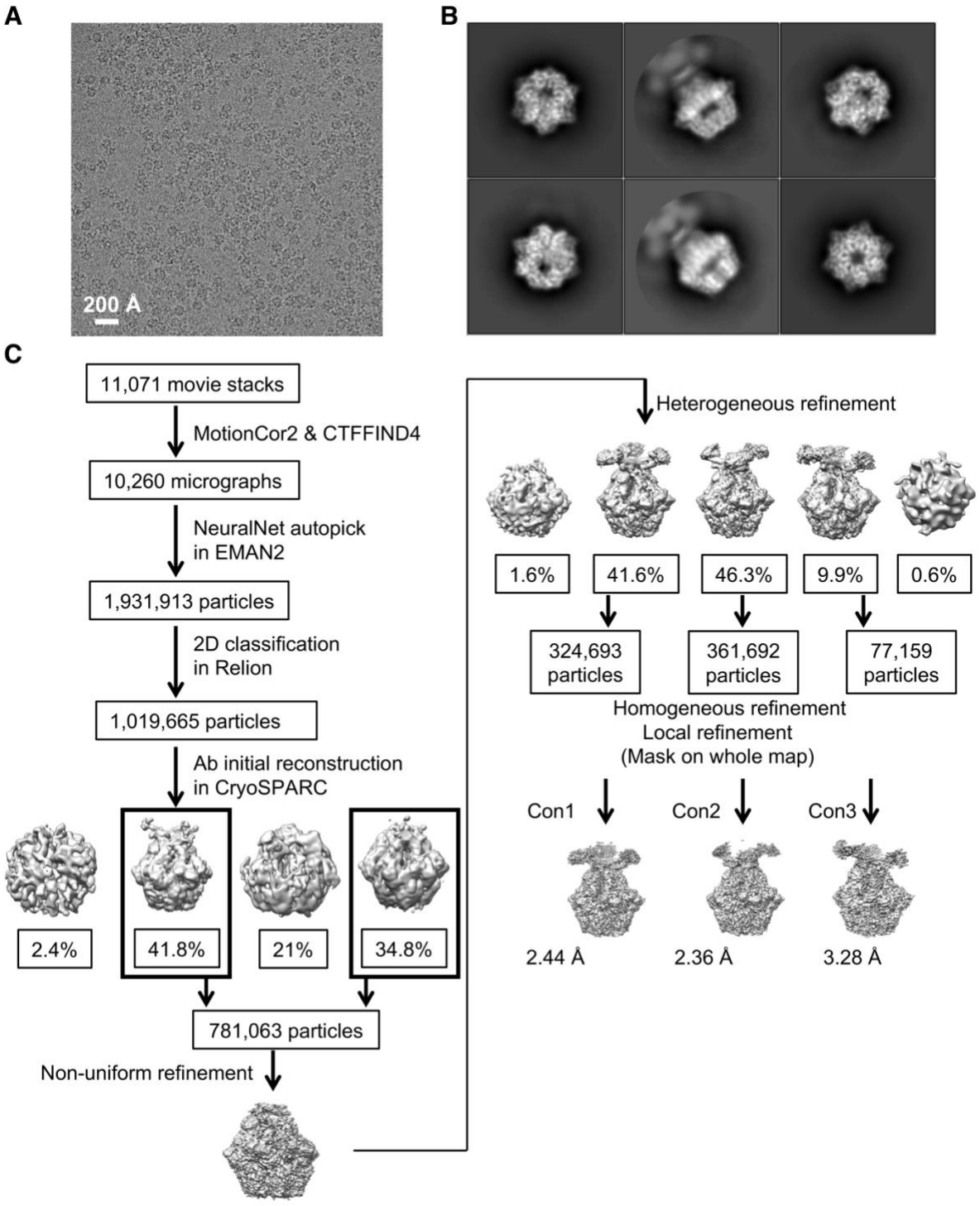

Fig. S1. Single-particle cryo-EM analysis of MtaLonA. (A) Representative motion-corrected cryo-EM micrograph. (B) Reference-free 2D class averages. (C) Workflow of the data processing.

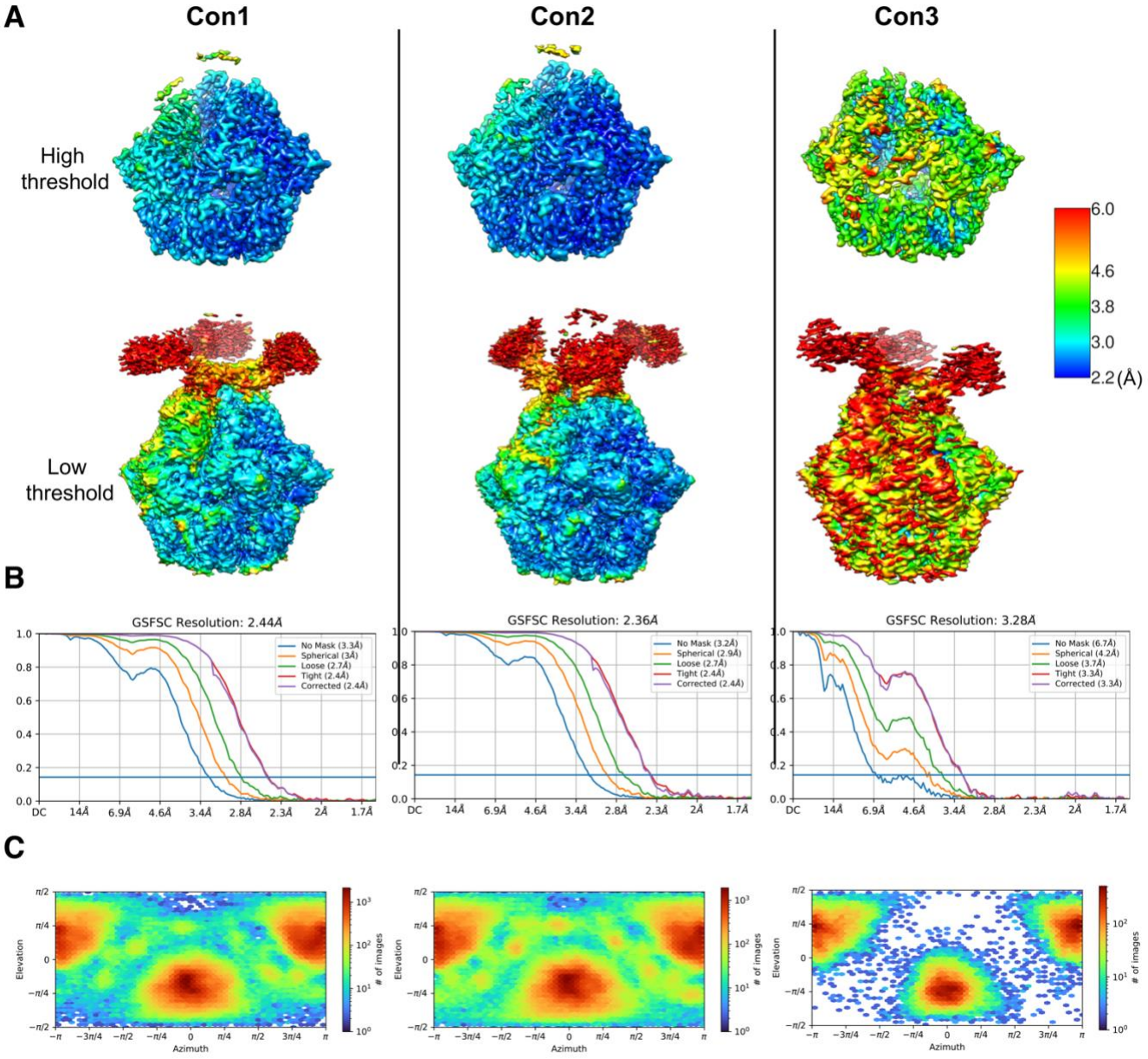

Fig. S2. Evaluation of the final 3D reconstructions of MtaLonA. (A) Resolution maps for the final 3D reconstructions in two threshold levels of Con1 (left), Con2 (middle), and Con3 (right). (B) Gold standard FSC plots for the 3D reconstructions of Con1 (left), Con2 (middle), and Con3 (right), calculated in cryoSPARC. (C) Euler angle distribution of the particle images.

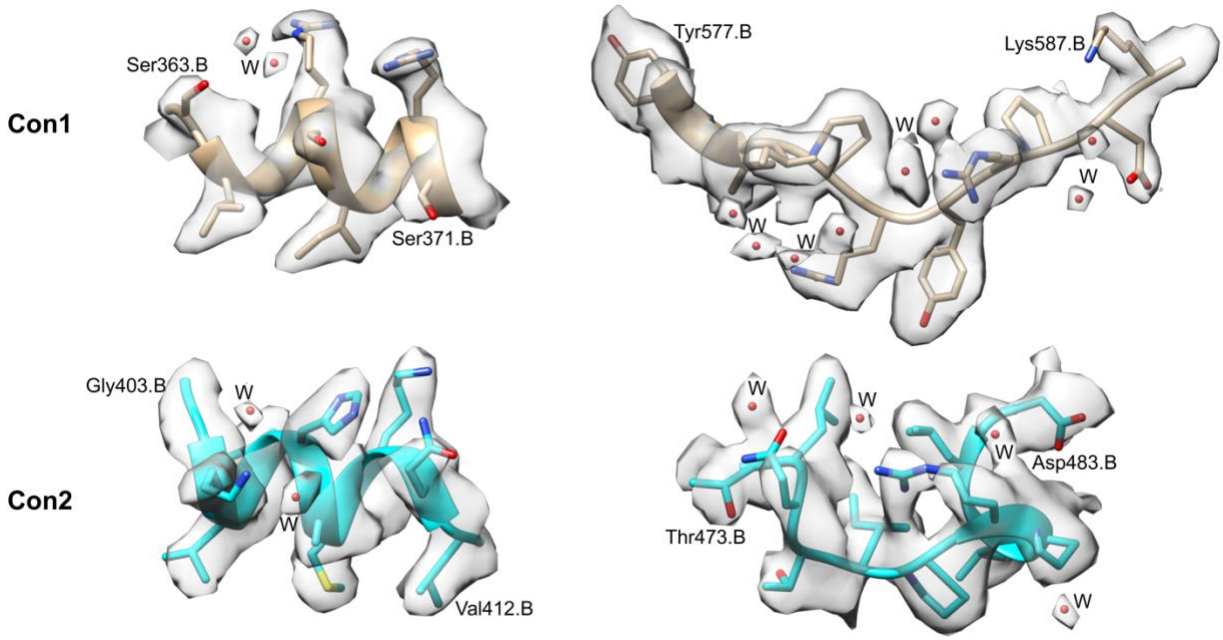

Fig. S3. Selected regions of the high-resolution maps showing well-defined densities for water molecules. The models are shown in ribbons and sticks, with water molecules (W) indicated. Selected side chains are labelled by residue name and number, followed by the chain ID.

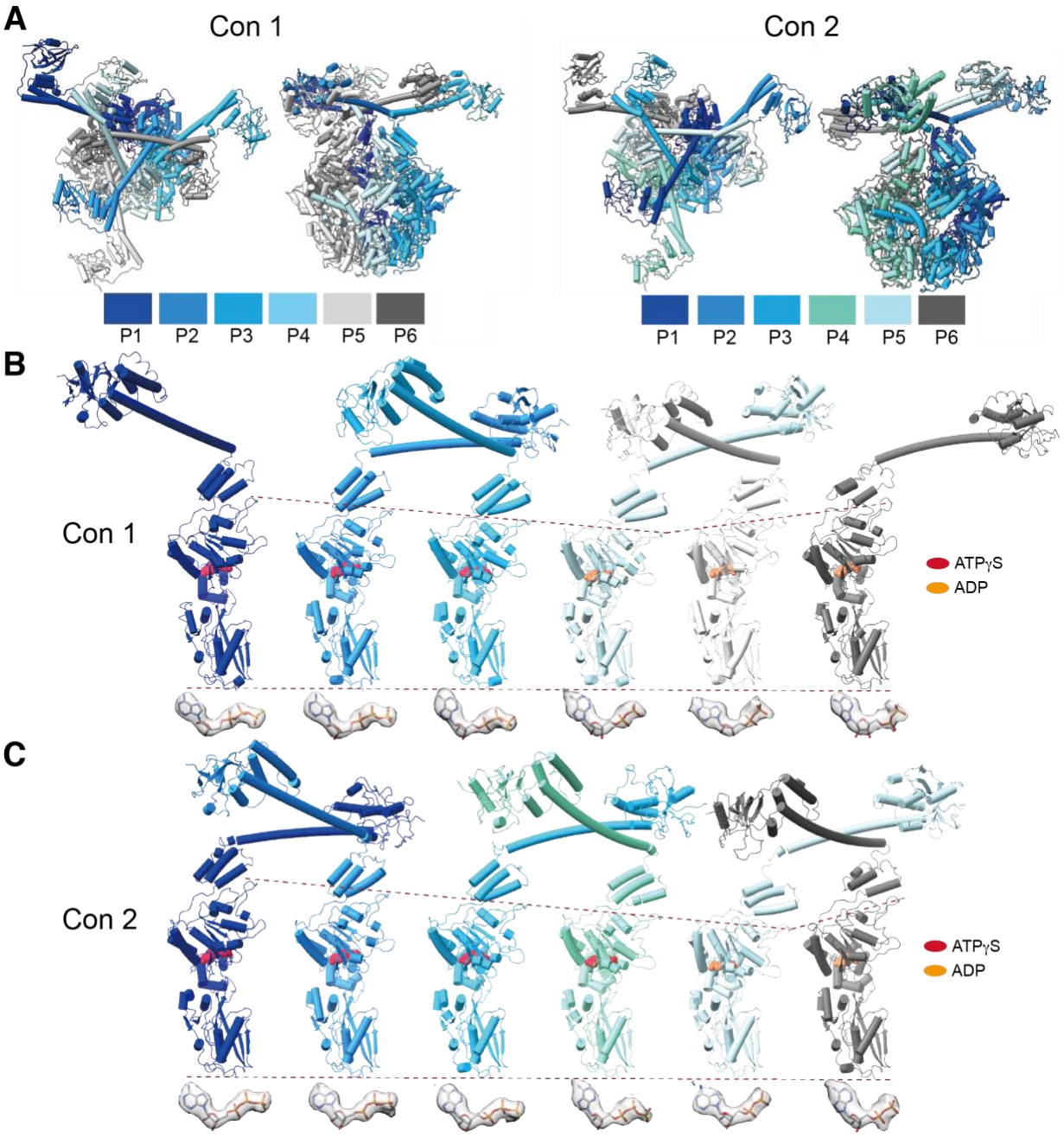

Fig. S4. Conformational states of MtaLonA bound to endogenous substrates. (A) Overall structures of Con1 and Con2 shown in ribbon models with cylindrical helices. (B and C) Aligned protomers of Con1 (B) and Con2 (C) showing different helical arrangements in the six conformational states (P1-6), of which the P5-P6 protomers in Con1 and the P6 protomer in Con2

serve as the seam subunits in the hexameric ring. The nucleotide densities with fitted models are shown below each of the protomers.

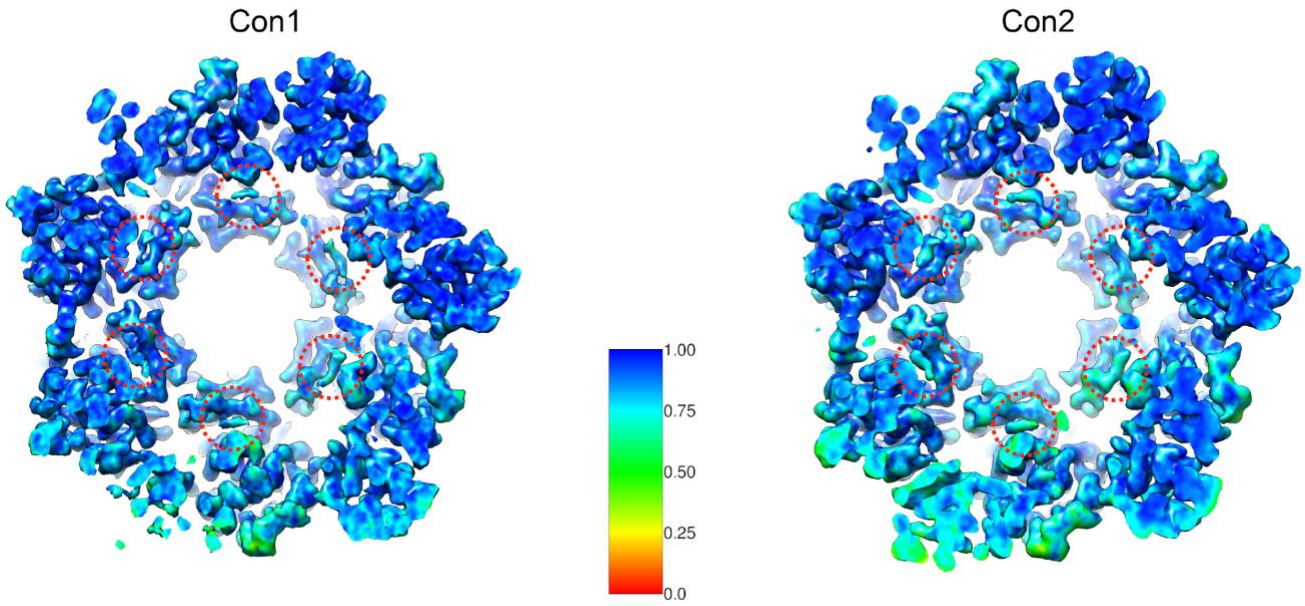

Fig. S5. Cryo-EM occupancy maps of Con1 and Con2. The cross-sectioned maps showing the substrate densities (red dashed circles) in the protease ring are colored according to the occupancy maps obtained by LocOccupancy (*22*). The occupancy ranges from 0 (red) to 1 (blue), indicating no density and full occupancy, respectively.

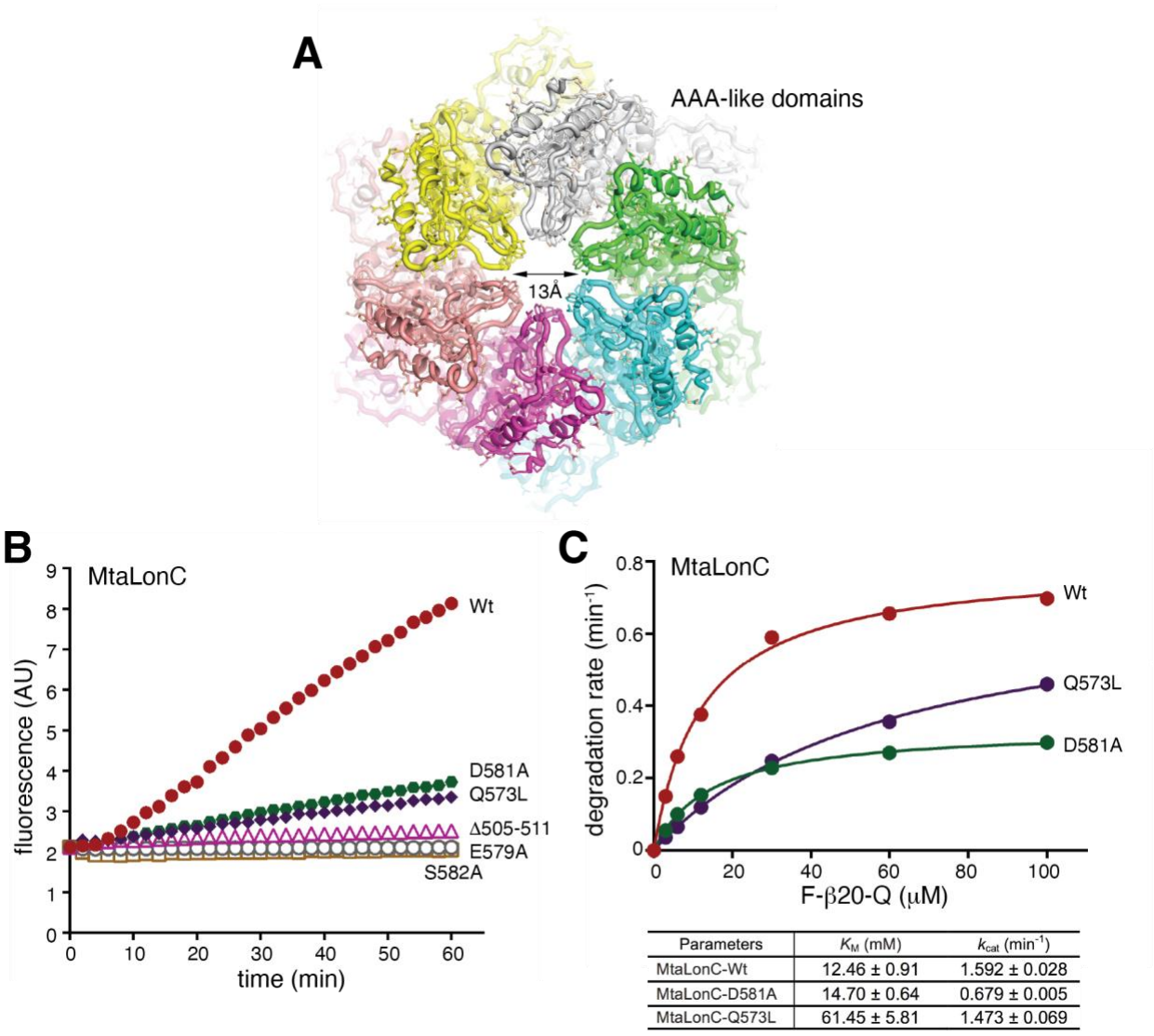

Parameters	K_M (mM)	k_{cat} (min^{-1})
MtaLonC-Wt	12.46 ± 0.91	1.592 ± 0.028
MtaLonC-D581A	14.70 ± 0.64	0.679 ± 0.005
MtaLonC-Q573L	61.45 ± 5.81	1.473 ± 0.069

Fig. S6. Structural and activity features of ATP-independent Lon-like protease MtaLonC. (A) Structure of MtaLonC showing the hexameric ring of AAA-like domains, which form an open pore for substrate access independently of ATP. (B) Peptidase activity of wild type (Wt) and mutants of MtaLonC. Cleavage of the intramolecularly quenched fluorogenic peptide F-β20-Q was monitored by real-time fluorescence detection. (C) Enzyme kinetic analysis of wild-type (Wt) MtaLonC and the mutants. Q573L and E579A are control mutants designed to alter the substrate-binding groove. The reactions were carried out by incubation at 55°C for 30 min and then stopped prior to fluorescence measurement.

Table S1. Cryo-EM data collection, processing, and model validation

	MtaLonA		
Data collection and processing			
Microscope	Titan Krios G3i		
Voltage (kV)	300		
Camera	Thermo Fisher Falcon 4		
Grids Type	R1.2/1.3 Quantifoil copper grid (200 mesh)		
Sample concentration	0.5 mg/mL		
Magnification	96,000×		
C2 aperture size (μm)	50		
Objective aperture size (μm)	100		
Pixel size (Å)	0.82		
Total exposure (e-/Å^2)	48		
Exposure time (s)	5.8		
Number of frames per exposure	40		
Energy filter slit width (eV)	N/A		
Data collection software	EPU 2.7		
Maximum image shift (μm)	6		
Number of exposures per hole	6		
Defocus range (μm)	-0.6 to -2.1		
Number of micrographs collected	11,071		
Number of micrographs used	10,260		
Number of initial particles	1,931,913		
Conformations	**Con1**	**Con2**	**Con3**
Symmetry	C1	C1	C1
Number of final particles	324,693	361,692	77,159
Resolution (0.143 gold standard FSC, Å)	2.44	2.36	3.28
Local resolution range (Å)	2-6	2-6	3-8
Atomic model refinement			
Software	phenix	phenix	phenix
Clashscore, all atoms	3.93	4.08	6.68
Poor rotamers (%)	0.36	0.89	0.31
Favored rotamers (%)	95.42	94.91	96.46
Ramachandran outliers (%)	0.17	0.15	0.26
Ramachandran favored (%)	94.15	95.69	92.82
MolProbity score	1.57	1.49	1.82
Bad bonds (%)	0.01	0.07	0.08
Bad angles (%)	0.08	0.07	0.12
PDB code	7FID	7FIE	7FIZ

Table S2. Crystallographic data collection and refinement statistics

Data collection				
Crystal (space group *P*6)	**S582A/F-β20-Q**	**S582A/β19**	**D581A/ F-β20-Q**	**D581A/β19**
Resolution range (Å)	30.0-2.12 (2.20-2.12)†	50.0-2.20 (2.28-2.20)	20.0-2.10 (2.17-2.10)	20.0-2.25 (2.33-2.25)
Cell dimensions (Å), *a = b, c*	115.6, 135.5	115.8, 135.5	115.8, 136.3	115.7, 136.0
Total observations	665,808	394,543	375,487	254,263
Unique reflections	58,112 (5,772)	52,084 (5,127)	57,412 (5,444)	48,531 (4,799)
Redundancy	11.5 (11.4)	7.6 (7.4)	6.5 (5.7)	5.2 (4.7)
Completeness (%)	99.9 (100.0)	99.7 (98.7)	95.3 (90.9)	99.2 (98.2)
I/σ(I)	21.5 (3.9)	26.6 (3.3)	29.8 (2.3)	23.7 (2.1)
R_{merge} (%)	11.3 (69.8)	8.6 (65.5)	5.7 (89.1)	6.3 (59.2)
Refinement				
Resolution (Å)	29.95-2.12	30.46-2.20	19.85-2.10	19.83-2.25
Reflections [> 0 *σ(F)*], working/test	52,163/2,934	46,727/2,655	46,326/2,600	38,857/2,255
R factor/R_{free}	0.184/0.218	0.182/0.211	0.154/0.178	0.153/0.193
R.m.s.d. bond lengths (Å)/ angles (°)	0.013/1.6	0.014/1.7	0.010/1.4	0.010/1.5
Average *B* factor (Å^2)/no. of atoms				
Protein	42.2/4,553	44.8/4,510	32.8/4,566	36.9/4,509
Substrate	34.2/33	38.9/34	30.8/42	29.0/34
Phosphate ion	32.5/5	33.2/5	24.5/5	29.5/5
Water	48.0/372	48.1/280	39.4/427	39.9/257
Ramachandran plot (%)				
Most favored	92.5	91.2	92.6	91.9
Additionally allowed	7.1	8.6	7.2	7.9
Generously allowed	0.4	0.2	0.2	0.2
Disallowed	0	0	0	0
PDB code	7EV4	7EUY	7EV6	7EUX

†Values in parentheses correspond to the highest resolution shell.